APPLIED ORGANOMETALLIC CHEMISTRY
Appl. Organometal. Chem. 2005; **19**: 1096–1100
Materials, Nanoscience and Catalysis
Published online 9 September 2005 in Wiley InterScience (www.interscience.wiley.com). DOI:10.1002/aoc.978

Phosphorized zirconium oxide nanoparticles

G. Vaivars*, Ji Shan, G. Gericke and V. Linkov

University of the Western Cape, Department of Chemistry, Private Bag X17, Bellville, 7535 Cape Town, Western Cape, South Africa

Received 1 April 2005; Revised 9 May 2005; Accepted 20 June 2005

In this work a simple method to phosphorize the surface of nanometric particles of crystalline zirconia is described. The reaction rate of phosphorization was regulated by adding acetic acid and the observed particle size was in the range 40–60 nm. A proton conductivity of the order of 10^{-3} S cm^{-1} was measured for phosphorized nanoparticle powder mixed with micro-fine teflon powder (3 : 1) at room temperature. Phosphorized nanoparticles are stable when dispersed in acetic acid and are suitable for composite material preparation. Copyright © 2005 John Wiley & Sons, Ltd.

KEYWORDS: proton conductivity; phosphorized zirconia; nanoparticles

INTRODUCTION

The application of proton-conducting solid electrolytes to ionic devices requires high conductivity and good stability. The direct methanol fuel cell (DMFC) is a technology that is receiving attention because it has specific advantages over hydrogen-based fuel cell systems. A liquid-feed proton exchange membrane (PEM) fuel cell would be more suitable for fuel cells in cars and portable applications due to its simplified handling and increased energy density. At present, perfluorosulfonic membranes (as DuPont Nafion) are used almost exclusively in a PEM fuel cell. Nafion is permeable to methanol transport, thereby reducing fuel cell efficiency. Recent research has approached the development of novel proton-conducting membranes in a variety of strategies. The presence of an inorganic component can reduce the dependence of the conductivity on relative humidity, reduce the methanol permeability and increase the mechanical strength.[1]

Zirconium phosphate could be the material of choice as a filler for large-scale applications due to its stability in a hydrogen—oxygen atmosphere, its low cost and its low toxicity. Low toxicity is potentially a very important factor for fuel cells, which are promoted as an environmentally friendly source of energy. For this reason it is not surprising that in 1961 zirconium phosphate was applied in fuel cells by Dravnieks and Bregman[2] and for glass fibre membrane impregnation by Alberti.[3] Zirconium phosphate has features of increasing conductivity, due to high proton mobility on the surface of its particles, and good water retention. The reduced methanol permeability of the polymer membrane while maintaining a high power density is obtained by impregnating it with zirconium phosphate.[1,4–7]

Various aspects of works done recently on the development of zirconium phosphate composite membranes for PEM fuel cell applications are surveyed by Savadogo.[8] Zirconium phosphate has been precipitated *in situ*, both electrochemically and chemically in the pores of an ionomer membrane for fuel cell applications. Grot and Rajendran[6] prepared a nanocomposite of Nafion with zirconium hydrogen phosphate, which was precipitated in Nafion matrix by *in situ* reaction of $ZrOCl_2$ and H_3PO_4 at 80 °C. Clearfield[9] reported some ways to increase the conductivity by substituting OH groups in α-layered zirconium phosphate with a sulfophenyl pendant group. Young-Taek Kim *et al.*[10] prepared composite membranes to maintain proton conductivity at elevated temperatures: layered zirconium sulfoarylphosphonate composites with Nafion and sulfopolyether ketone;[13] zirconium phosphate composites with sulfonated polyetherketone;[11,12] and sulfonated poly(ether ether ketone).[12] These methods show some limitations and the use of zirconium phosphate nanoparticles might allow more efficient control of the pore size and density of the material. Vaivars *et al.*[14] prepared inorganic proton-conducting membranes for DMFCs by impregnating an inorganic porous substrate with zirconium oxide particles and by subsequent phosphorization. Carriere *et al.*[7] have shown that crystalline nanometric zirconium oxide is a good substrate for organic grafting via the zirconium phosphate bond.

*Correspondence to: G. Vaivars, University of the Western Cape, Department of Chemistry, SA Institute for Advanced Materials Chemistry, ESKOM Center for Electrocatalysis, Private Bag X17, Bellville, 7535 Cape Town, Western Cape, South Africa.
E-mail: gvaivars@uwc.ac.za
Contract/grant sponsor: ESKOM Center for Electrocatalysis.

In this work a simple method to modify the surface of nanometric particles of crystalline zirconia is described. The modified particles were produced for composite polymer membrane preparation.

EXPERIMENTAL

Chemicals

Phosphoric acid and acetic acid were purchased from Aldrich Chemicals, ZrO_2 sol was purchased from Johnson Matthey and zirconium oxide nanoparticle powder was purchased from Degussa (average particle size 12 nm).

Measurements

X-ray powder diffraction (XRD) patterns were obtained with a Shimadzu XD-3A diffractometer using Ni filters and Cu K_α radiation at 30 kV and 30 mA. Infrared spectra (IR) were recorded on a Perkin Elmer Paragon 1000 FTIR spectrophotometer using the KBr pellet method (95 wt.% KBr). Samples for XRD and IR measurements were ground in an agate mortar and dried for 24 h at 100 °C. The surface area of the powdered samples was determined through the BET technique using a Micromeritics Accelerated SA and Porosimetry (ASAP) 2010 system.

Transmission electron microscopy (TEM) pictures were obtained using a Jeol electron microscope. First the sample was ground into a fine powder, which was then suspended in methanol, placed on a carbon-coated copper grid and sealed with a polymer (5% Butyar in chloroform). For taking high-resolution pictures a Hitachi H7500 TEM instrument was used, operating at 120 kV.

Impedance measurements of each sample were conducted using an Autolab potentiostat/galvanostat PGSTAT30 in combination with a computer-controlled frequency response analyser over a frequency range of 0.1–100 00 Hz. Disks with a diameter of 1 cm and a thickness of 0.2 cm were pressed from powdered samples at 1500 MPa. A cell with a serpentine flow field was used to measure the conductivity of the membrane. The sample to be characterized was pressed between two porous carbon cloth layers, which were used as electrodes. The volume resistance was obtained from a Cole–Cole plot by extrapolating to high frequencies using Autolab software.

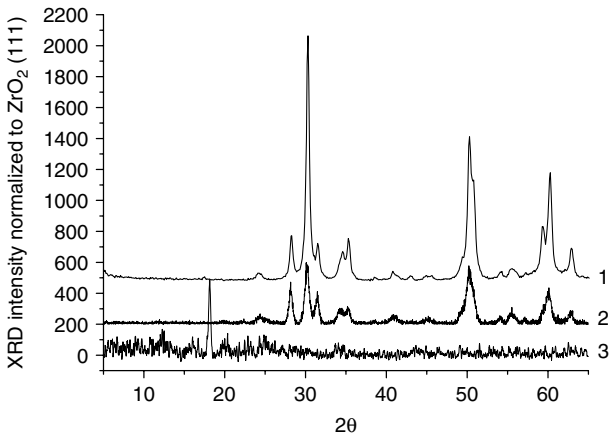

Figure 1. X-ray diffraction pattern of ZrO_2 nanoparticle powder (1) and phosphorized ZrO_2 powders from ZrO_2 nanoparticle suspension (2) and ZrO_2 sol (3).

RESULTS AND DISCUSSION

Zirconium phosphate synthesis and XRD analysis

Zirconium phosphate suspension was prepared as follows:

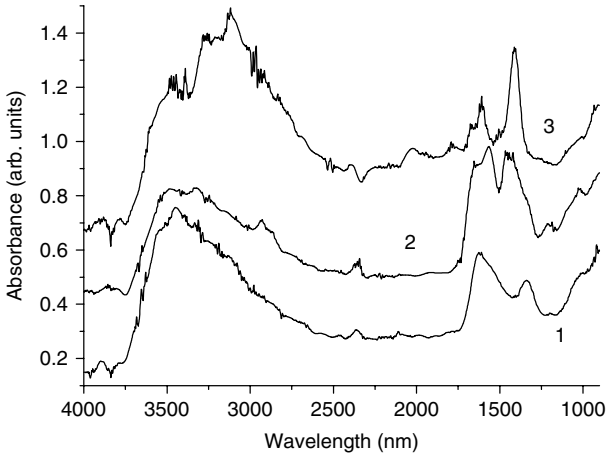

Figure 2. Infrared spectra of ZrO_2 powders prepared by drying from: nanoparticle suspension in water (1); nanoparticle suspension in acetic acid (2); sol (3).

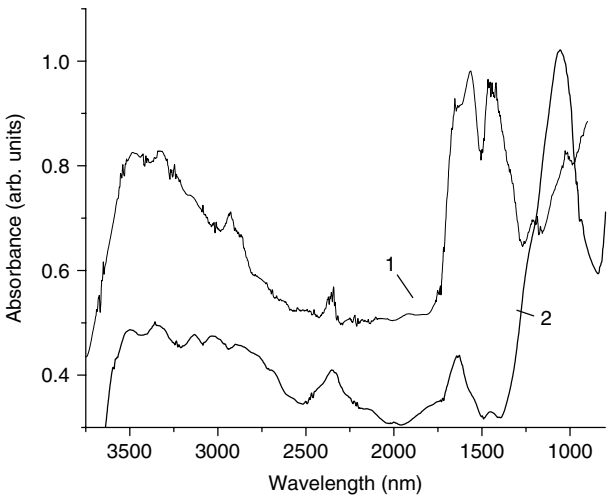

Figure 3. Infrared spectra of ZrO_2 powders prepared from a nanoparticle suspension (1) and a phosphorized nanoparticle suspension (2).

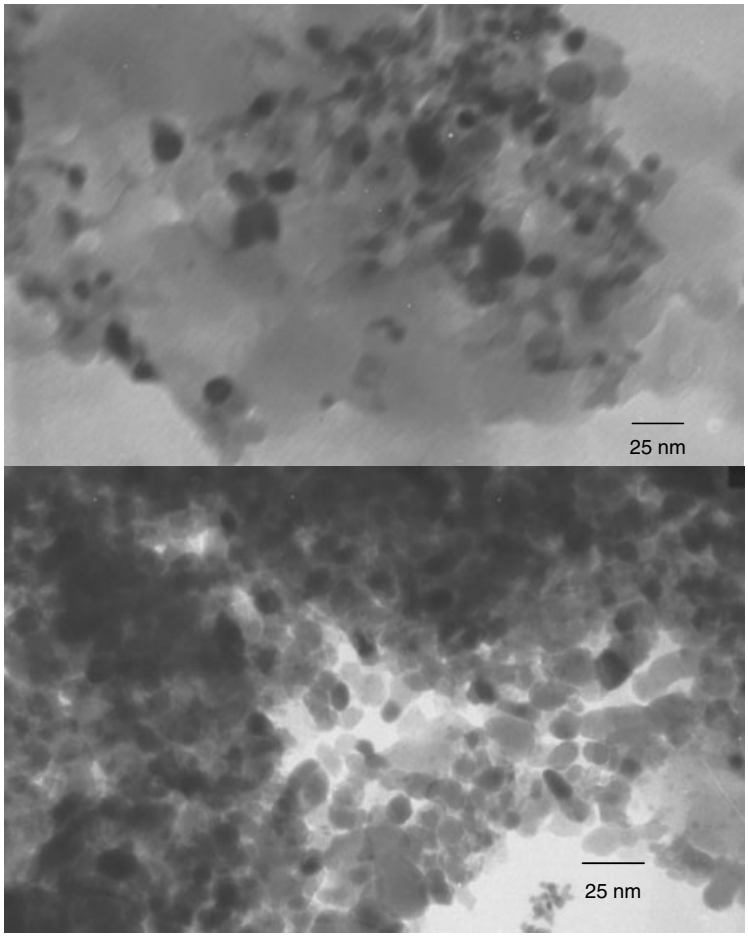

Figure 4. Transmission electron micrographs of ZrO_2 nanoparticles before (bottom) and after phosphorization (top).

(i) Procedure I, from sol: the 2 M acetic acid solution was added dropwise to the 20 wt.% ZrO_2 sol (purchased from Johnson Matthey 1 : 1) and the resulting mixture was stirred for 30 min using a magnetic stirrer. An 8% phosphoric acid solution (ZrO_2–phosphoric acid, 1 : 2) was added, heated to 80 °C in an oven and cooled down to room temperature.
(ii) Procedure II, from suspension: a ZrO_2 nanoparticle suspension was prepared by mixing 3 g of ZrO_2 nanoparticle powder (from Degussa) with 97 g of 2 M acetic acid solution. The mixture was stirred with a magnetic stirrer until a milky solution was obtained and mixed with 8% phosphoric acid solution (ZrO_2–phosphoric acid, 1 : 2). The mixture was slowly heated up to 80 °C and cooled down to room temperature.

Zirconium phosphate suspension was vacuum dried and the resulting product was a paste (10–20% zirconium phosphate content) that was used for composite electrolyte preparation.

For analytical purposes, zirconium oxide and zirconium phosphate dispersions (from Procedure I and II) were dried in an oven at 80 °C. The final product was crushed into a fine powder in an agate mortar. For conductivity measurements, zirconium phosphate powder was mixed with micro-fine Teflon powder (3 : 1) and pressed in a press-form to form discs.

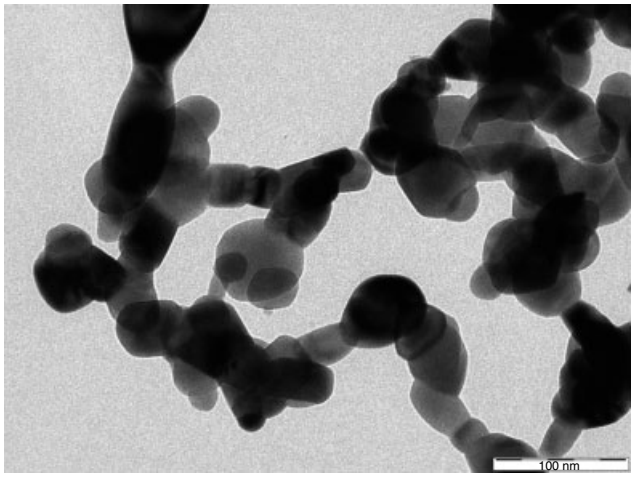

Figure 5. Transmission electron micrograph of phosphorized ZrO_2 nanoparticles.

Powder X-ray diffraction measurements of zirconia sol particles after phosphorization (Procedure I) yielded an amorphous pattern with a few weak reflections of crystalline α-zirconium phosphate (Fig. 1, curve 3). During treatment all zirconia sol particles reacted with phosphoric acid solution. In the case of phosphorized zirconia nanoparticles the X-ray diffraction pattern is different. It is still characteristic of zirconia nanoparticles without any change in diffraction domains (Fig. 1, curve 1 and 2) or broadening of the diffraction peaks. At the same time, the surface coverage with phosphate groups and zirconium phosphate formation is confirmed by IR spectroscopy.

FTIR Spectra

Figure 2 shows the FTIR spectra of ZrO_2 powders prepared from a nanoparticle suspension in water (curve 1), a nanoparticle suspension in acetic acid (curve 2) and sol (curve 3). The powders are hygroscopic and the water content is characterized by broad water bands at 2700–3700 cm^{-1}. The presence of acetic acid was important in order to regulate the rate of phosphatization and to prevent the agglomeration of phosphated particles. The acetic acid is characterized by a strong band at 1750 cm^{-1} that is not presented in Fig. 2 or Fig. 3, suggesting that the acetic acid is removed during drying. After phosphorization, the main P–O stretching band at 1050 cm^{-1} is observed (Fig. 3, curve 2).

Phosphorized sol particles formed a low-crystalline mass of large, agglomerated particles with a diameter up to 1 μm.

Slow phosphorization of nanoparticles prevents the formation of a homogeneous mass. The TEM pictures (Fig. 4) show a uniform size distribution for nanoparticles. After phosphorization some increase of particle size is observed. The observed size of particles is in the range 40–60 nm (see also high-resolution TEM picture in Fig. 5).

Conductivity measurements

Impedance spectroscopy was carried out to determine the proton conductivity of zirconium phosphate powders. Zirconium phosphate is a well-known surface conductor and its conductivity is strongly promoted by the presence of absorbed water. The high proton conductivity (0.01–0.1 S cm^{-1} at room temperature) of the pressed nanoparticle powder arises from protonic transport in a large number of water molecules adsorbed on the nanoparticle surface. To reduce the impact of adsorbed water, Teflon powder was added. According to the BET measurements, phosphorized nanoparticle powder gives a higher surface area than the powder prepared from sol (Table 1) and the observed conductivity values are lower. Phosphorized nanoparticles are well-defined crystalline particles (Fig. 5) whereas phosphorized sol particles form an amorphous mass. The Teflon powder blocks the particle surface from adsorbing water more efficiently in the case of phosphorized nanoparticles. For both samples the Teflon additive reduced the conductivity of powder to the level of 10^{-3}S cm^{-1}, which is typical for α-zirconium phosphate. An opposite effect was observed during the formation of polymer composite. In this case, the particles interact with the polymer host and phosphorized ZrO_2 nanoparticles are used as better promoters of the proton transfer.

Table 1. Proton conductivity and BET surface area of phosphorized ZrO_2 particles

Powdered samples	Conductivity at (mS cm^{-1})20 °C	BET surface area, (m^2g^{-1})
Phosphorized ZrO_2 sol particles	9.6	4 ÷ 6
Phosphorized ZrO_2 nanoparticles	3.8	16

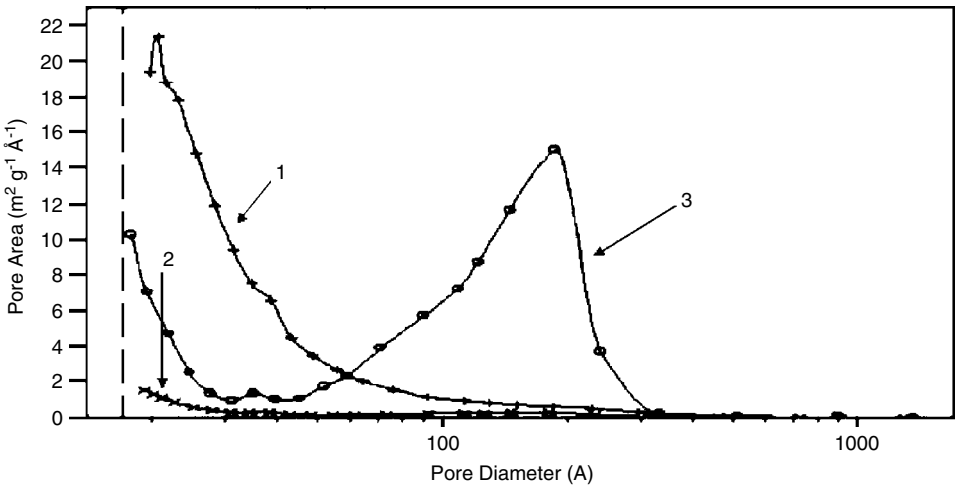

Figure 6. Pore size distributions of ZrO_2 nanoparticle powder (1), ZrO_2 nanoparticle powder dispersion in acetic acid solution (2) and phosphorized ZrO_2 nanoparticle suspension (3) based on pore area versus pore diameter.

Figure 6 gives a comparison of pore size distribution based on the pore area of the ZrO_2 nanoparticle powder (1), the ZrO_2 nanoparticle powder dispersion in acetic acid solution (2) and the phosphorized ZrO_2 nanoparticle suspension (3). The nanoparticle powder showed a high surface area with a small pore diameter. The dispersion in acetic acid decreased the pore area, and after treatment with phosphoric acid solution a characteristic high-intensity peak with a maximum at 20 nm was observed.

CONCLUSIONS

The described method of ZrO_2 phosphorization to produce proton-conductive zirconium phosphate particles is suitable for nanoparticle powder phosphorization but was not effective in the case of the ZrO_2 sol. The Phosphorized nanoparticles produced (diameter 40–60 nm) are stable and suitable for composite membrane preparation.

Acknowledgements

The authors wish to thank Professor Helmut Bönnemann (Max-Planck-Institut für Kohlenforschung, Mülheim ad Ruhr) for the TEM measurements. The ESKOM Center for Electrocatalysis is acknowledged for financial assistance.

REFERENCES

1. Jones DJ, Roziere J. *J. Membr. Sci.* 2001; **185**: 41.
2. Dravnieks A, Bregman JI. *Chem. Eng. News* 1961; **39**: 40.
3. Alberti G. *Atti. Accad. Naz. Lincei Cl. Fis. Mater. Nat. Rend.* 1961; **31**: 427.
4. Costamagna P, Yang C, Bocarsly AB, Srinivasan S. *Electrochim. Acta* 2002; **47**: 1023.
5. Yang C, Costamagna P, Srinivasan S, Benziger J, Bocarsly AB. *J. Power Sources* 2001; **103**: 1.
6. Grot WG, Rajendran G. US Patent 5,919,583, 1999.
7. Carriere D, Moreau M, Lhalil K, Barboux P, Boilot JP. *Solid State Ion.* 2003; **162**: 185.
8. Savadogo O. *J. Power Sources* 2004; **127**: 135.
9. Clearfield A. *Curr. Opin. Solid State Mater. Sci.* 1996; **1**: 268.
10. Young-Taek Kim, Min-Kyu Song, Ki-Hyun Kim, Seung-Bae Park, Sung-Kyu Min, Hee-Woo Rhee. *Electrochim. Acta* 2004; **50**: 642.
11. Ruffmann B, Silva H, Schulte B, Nunes SP. *Solid State Ion.* 2003; **162**: 269.
12. Nunes SP, Ruffmann B, Rikowski E, Vetter S, Richau K. *J. Membr. Sci.* 2002; **203**: 215.
13. Alberti G, Casciola M. Palombari R. *J. Membr. Sci.* 2000; **172**: 233.
14. Vaivars G, Mokrani T, Hendricks N, Linkov V. *J. Solid State Electrochem.* 2004; **8**: 882.

